Journal of Structural Geology, Vol. 5, No. 3/4, pp. 329 to 339, 1983
Printed in Great Britain

0191-8141/83 $3.00 + 0.00

Estimation of volume changes by comparative chemical analyses in heterogeneously deformed rocks (folds with mass transfer)

J. P. GRATIER

I.R.I.G.M. University of Grenoble, B.P. 68, 38402 St Martin d'Hères Cedex, France

(*Received* 21 *June* 1982; *accepted in revised form* 28 *February* 1983)

Abstract—This paper presents a method for calculating the volume change between the various sectors of the same heterogeneously deformed layer (fold, shear zone) by comparing the chemical composition of deformed sectors with that of a reference sector. The principle consists of considering some minerals as being insoluble (illite, chlorite) and passively concentrated in deformed zones because of the loss of more soluble minerals (quartz, calcite, dolomite) by pressure-solution.

Simple observations can be used to test the validity of the assumptions required to calculate volume change (Δ). In the analysis of a slaty matrix around a ptygmatic fold, a map of Δ values is drawn and these Δ values are shown to be compatible with the general strain pattern.

For several limb–hinge pairs of straight-limbed folds, the relations between volume change (Δ), elongation parallel to limb layering ($\Delta l/l_o$) and the angle between limb and hinge (α) are determined. The influence of various parameters (such as temperature, pressure, initial composition and structure of the rock) on these relations, is also pointed out.

INTRODUCTION

ONE OF the main objects of the study of natural rock deformation is to restore the state of the rocks to before they were deformed. For this purpose, finite deformation values and orientations must be estimated for any point of a deformed area by means of strain markers such as fossils, conglomerate pebbles, or discontinuity planes (Ramsay 1967). In most cases, the values and orientations of strain vary from point to point; the deformation is heterogeneous. To unstrain such structures, the simplest method is to divide the whole heterogeneously deformed area into small elements whose deformations are assumed to be homogeneous (Schwerdtner 1977, Cobbold 1979). Each element is then individually unstrained. A set of blocks (representing the initial state of each element) fitting more or less together is thus obtained. Then, a mathematical method can be used to achieve the best fit between the various blocks so as to restore the initial state of the studied area (Percevault & Cobbold 1982, Cobbold & Percevault, this issue).

The problem is finding strain markers to estimate strain values. It is still more complicated when deformation occurs with a volume change, making it difficult to estimate deformation by means of geometric markers (Ramsay 1967). However, this case is comparatively frequent in natural deformations with mass transfer, for example by pressure-solution (Kerrich 1977). Volume changes may be substantial and amount to over 50% of the initial rock volume (Gratier 1976).

This paper present a method of estimating the volume changes between various zones of the same heterogeneously deformed layer (fold, shear zone, deformed matrix around a rigid object) by comparing the chemical compositions of the zones.

PRINCIPLES AND LIMITS OF THE VOLUME CHANGE DETERMINATION METHOD

The principle of this method has already been described (Gratier 1979, 1982). It can be summarized as follows. It is assumed that a rock undergoing mass-transfer deformation (for example by pressure-solution) can be classified into two parts.

Part 1 is composed of soluble mineral elements (calcite, quartz, dolomite, etc.) which leave the zones undergoing maximum compressive stress (named 'exposed zones'). These materials may be redeposited or not redeposited in the zones undergoing minimum (often tensile) stress (named 'protected zones').

Part 2 is composed of insoluble minerals (micas, chlorites, etc.) which are passively concentrated (because of mobile-material loss) in the zones subject to maximum compressive stress (Barrouquere *et al.* 1969, Williams 1972, Durney 1972, Gray 1977, Delair & Leroux 1978).

Thus, when two sectors (e.g. fold limb and hinge) located in an initially homogeneous layer and undergoing heterogeneous stress (Stephansson 1974) have been deformed by pressure-solution, they reveal a difference in chemical compositions.

Schematically, for the example of Fig. 1, the mass decrease of the exposed sector (limb) compared with the protected sector (hinge = M_o) is:

$$\Delta M/M_o = (I_p/I_e) - 1 = -0.17 \quad (-17\%),$$

I_e and I_p being the total percentages of all insoluble minerals in the exposed zone (I_e) and in the protected zone (I_p). The mass decrease of each soluble mineral is:

$$\Delta M'/M'_o = (I_p/I_e)(M_e/M_p) - 1,$$

M_p and M_e being the percentages of each soluble mineral

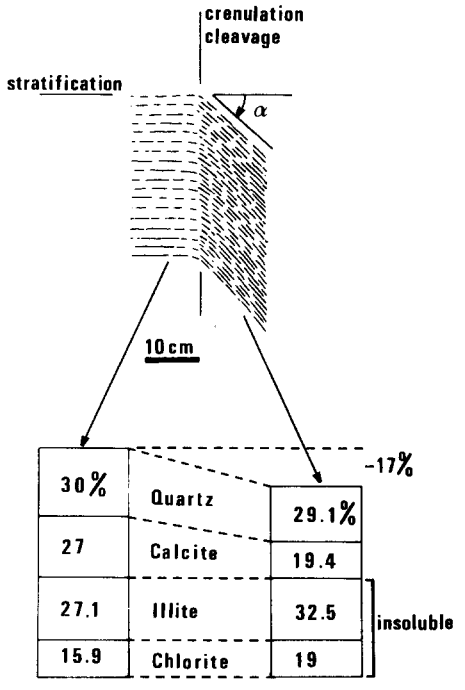

Fig. 1. Determination of the mass change, within a layer, between limb and hinge of a fold. After a few simple tests have been carried out (see text and Figs. 2 and 3) illite and chlorite are considered as being insoluble minerals, passively concentrated in the fold limb, by the loss of mobile elements by pressure-solution (quartz, calcite, dolomite). Mass decrease $\Delta M/M_0 = (I_p/I_e) - 1 = -0.17\,(-17\%)$, is calculated in the limb compared with the hinge; I_p being the sum of insoluble elements in the hinge and I_e the sum of insoluble elements in the limb. The mass decrease of quartz is −19%, and that of calcite −40% (see text). In this case, the hinge is considered as the initial state, and the hinge–limbs pair an open system (see Figs. 4 and 7). This fold is represented by a triangle with point in Fig. 7.

in the exposed sectors (M_e) and protected sectors (M_p). Thus, a 40% loss for calcite and a 19% loss for quartz are observed when the limb is compared with the hinge in Fig. 1.

These results can be obtained only because a number of hypotheses are adopted for simplification. Before all the results and their applications are given, the validity of these hypotheses and the consequences of the non-validity of some of them on the accuracy of the values obtained, will be discussed.

Initial chemical homogeneity of layers

In order to probe the presence of variations in chemical composition within the same layer, a horizontal layer undergoing sudden dip changes (straight-limbed fold) has been taken as an example. Analyses reveal a great steadiness in the composition of horizontal parts as well as extremely varied compositions in limbs according to the angle α between hinge and limb (Fig. 3).

Calculation of mineral composition in a rock

In current analyses, the chemical composition of rocks is generally expressed in element or oxide contents. Some of these elements (such as Si) which are present both in highly soluble minerals (quartz) and slightly soluble ones (micas, chlorites) are not easy to interpret in terms of mineralogical composition. Direct modal analysis was not possible for the rocks concerned here, because of the very small size of the mineral. Thus, in addition to the chemical composition of the rocks (expressed in oxide contents) it is necessary to know which minerals are present by X-ray diffraction analysis, as well as their chemical formulae. By using a programme of computation by successive iterations, it is possible to determine the mineralogical composition best fitted to particular element contents (Buffet 1981). Some sources of inaccuracy comes from this successive process:

(i) errors in initial analysis (of the order of a few percent if analyses of the same rock carried out by different laboratories are compared);

(ii) errors linked with approximations in the chemical formulae of minerals and

(iii) errors linked with the elimination of some minerals which had not been identified by X-rays analysis.

As the present work was carried out on a series of samples of the same rock, deformed in various ways but containing the same minerals and analysed by the same laboratory, most of these errors cancel out.

Influence of mineral recrystallization

As described by several writers (Etheridge & Hobbs 1974, Boulter & Raheim 1974, Stephens *et al.* 1979), mineral recrystallizations (of micas or chlorites) sometimes appear in exposed zones. The result may be material transfer between exposed zones and protected zones if the recrystallization occurs with a change in mineral composition (Vernon 1977, Wilson & Bell 1979, Caron *et al.* 1981). In exposed zones, concentrations of some elements may be added to the passive concentrations of insoluble minerals during the pressure-solution process. According to Knipe (1981), two transformations seem particularly important: the recrystallization of illite into phengite, with increase in K, Si, Fe and Al and decrease in Na, and the recrystallization of chlorite accompanied by increase in Al and decrease in Fe. In both cases, however, we may consider that the concentrations due to these recrystallizations are not identical for all the elements concerned. Therefore, one possible way of testing the magnitude of these material transfers due to recrystallization is to compare the evolution of the content of the various elements of the same rock subject to increasing deformation. More precisely, in a series of samples taken from the same folded layer (e.g. Fig. 5a), the horizontal bedding sample (or hinge) is considered as a protected zone and the other samples (limbs) are considered as exposed zones becoming more and more intensely deformed as the layer dip (β) increases.

The $X(p)/X(e)$ ratio is called $R(X)$, $X(p)$ being the content of one element X in the protected zone and $X(e)$ the content of the same element in an exposed zone. The ratio $R(Al) = Al(p)/Al(e)$ is taken as a reference (only because Al is the most abundant of the least mobile elements). Thus, the evolution of the ratio normalized

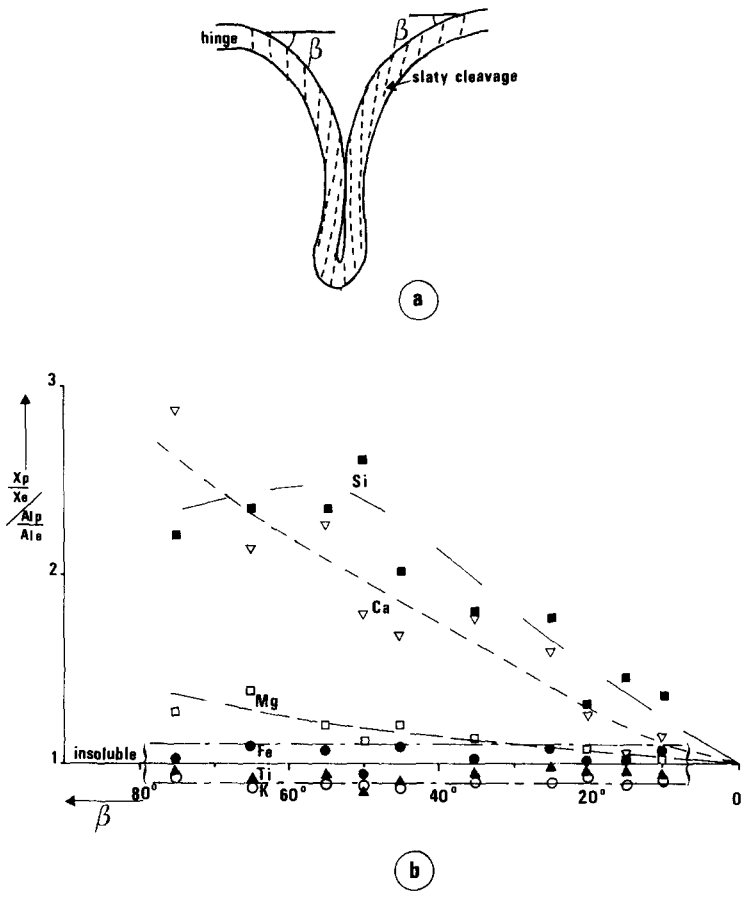

Fig. 2. Mobility test of elements Si, Ca, Mg, Fe, Ti and K (compared with a reference element Al) along a folded layer, as the layer dip (β) increases. (a) Fold example (Fig. 5). (b) Evolution of the ratio X(p)/X(e) to Al(p)/Al(e) with angle β. X(p) and X(e) are the concentrations of an element X in the protected zone (hinge) and in exposed zones (limbs), and Al(p) and Al(e) the respective concentrations of Al. Elements whose ratios vary from 0.9 to 1.1 (variation due to various inaccuracies, see text) without any perceptible evolution as deformation and β increase are considered to be contained in insoluble minerals. The calculated Δ values are given in Fig. 5.

as $R(X)/R(\mathrm{Al})$ may be related to angle β (layer dip for each sample) as plotted in Figs. 2 and 3. Two different type of behaviour clearly appear.

(i) In some cases (Fig. 2), several elements (Fe, K, Ti) show a good stability of the ratio $R(X)/R(\mathrm{Al})$ between 0.9 and 1.1 without significant change with angle β, and therefore strain intensity. However, for other elements such as Mg and especially Ca and Si, this ratio significantly increases as β increases. In such cases, if recrystallization takes place in exposed zones, elements such as Fe, Ti, K and Al will recombine on the spot, whereas Si, Ca and Mg leave the zones. Some minerals such as illite, chlorite, pyrite, and Ti oxide may then be considered as being insoluble (or passive), whereas quartz, calcite and dolomite are soluble (or mobile).

(ii) In other cases (Fig. 3), for almost all the elements, there is an evolution of the ratio $R(X)/R(\mathrm{Al})$ as deformation increases. As dip increases, a slight decrease for K or Na, and an increase for Fe, Mg, Si and Ca are observed. Some recrystallization probably appears with transfer of some elements in exposed zones but the interpretation of this transfer is still being carried out. Thus, for the calculation of volume changes due to pressure-solution, only passive minerals which contain elements whose ratios $R(X)/R(\mathrm{Al})$ do not exceed the variations due to analysis inaccuracies are used. A variation of $\pm 10\%$ is chosen. In one of the examples presented (Fig. 3b), only illite and Ti oxide are considered as being insoluble, whereas in the other examples (Figs. 2 and 3c) chlorite, pyrite, Ti oxide and illite are consideredinsoluble. The content in Na being very low and irregular, it was not taken into account for Δ calculations.

Equivalence of mass change with volume change

In the example of Fig. 1, the mass change between the exposed zone and protected zone is calculated. For this mass change to be equated with volume change, it must be demonstrated that the density of the two zones is constant. Otherwise, a correction factor (Fd) must be introduced to take into account the difference of density between two differently deformed zones,

$$\Delta = \Delta V/V_0 = (\Delta M/M_0)Fd.$$

To estimate this correction factor, measurements of density were made along a folded layer which presented a clear chemical differentiation ($\Delta M/M_0 = -50\%$) between exposed and protected zones (respectively

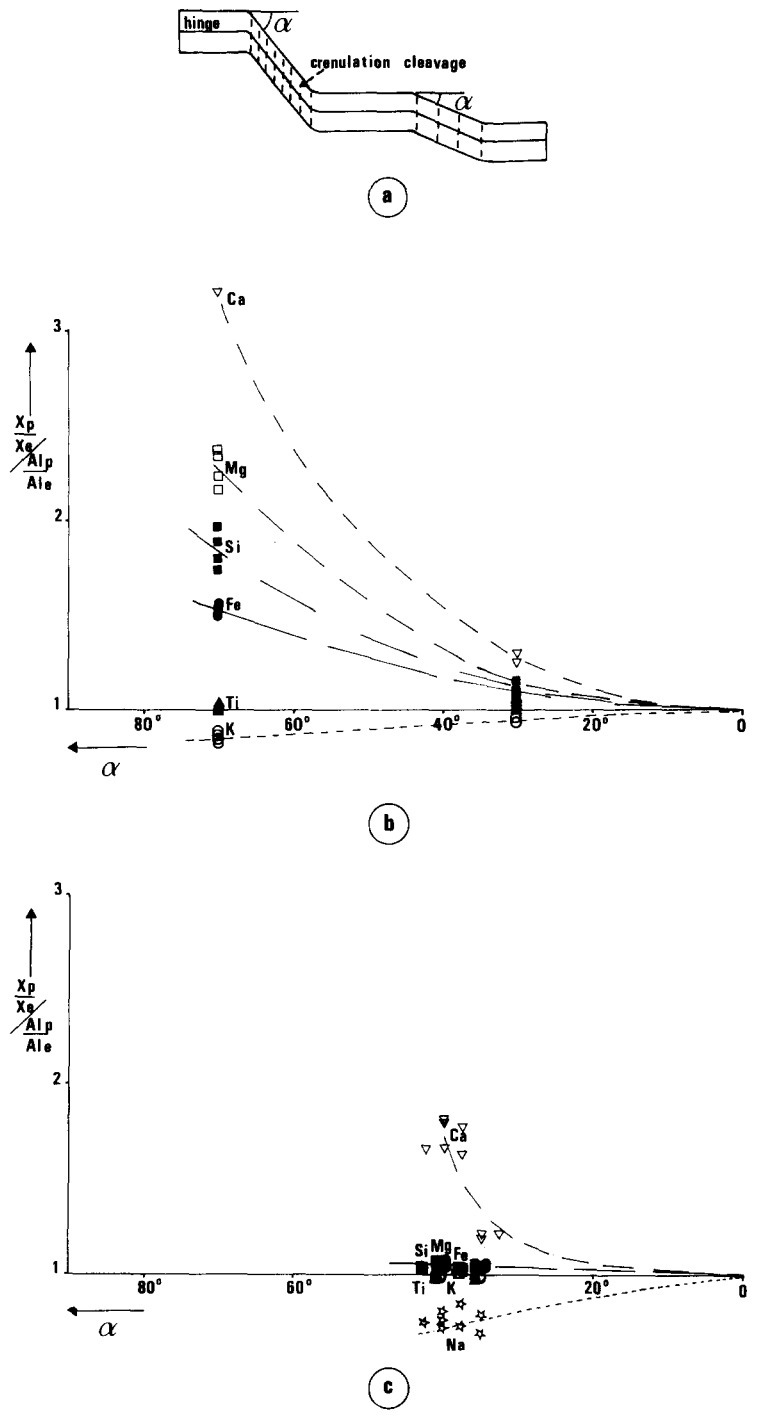

Fig. 3. Mobility test of various elements (compared with a reference element Al) in two limb–hinge pairs of straight-limbed folds, as the limb–hinge angle (α) increases. (a) is the fold sketch and (b) and (c) the evolution of the ratio $X(p)/X(e)$ to Al(p)/Al(e) with angle α, as in Fig. 2. Elements whose ratios vary from 0.9 to 1.1 are considered to be contained in insoluble minerals. The Δ values for each limb–hinge pair of (b) are given in Fig. 7 (black squares), and in Fig. 9(a). The Δ values for (c) are given in Fig. 7 (black triangles), and in Fig. 9(b). The size of the limb–hinge pair varies from 1 cm to 1 dm.

situated near the intrados and the extrados of an adjacent folded layer, see Figs. 5a & c). The mean density for the exposed zones was $d = 2.762 \pm 0.01$, and for the protected zones was $d = 2.742 \pm 0.004$. The difference of density (less than 1%) was thus an order of magnitude less than the value of the mass transfer. The value of the correcting factor may therefore be taken as equal to 1 without introducing too much inaccuracy in the Δ values.

Mass transfer and deformation models

The arguments here are based on the particular case of volume change in a shear zone, selected for its simplicity and because it is a good model for deformation in straight-limbed folds. The volume change is achieved through a decrease in the shear-zone thickness (Ramsay 1980). For a hinge–limb pair such as that in Fig. 4, two

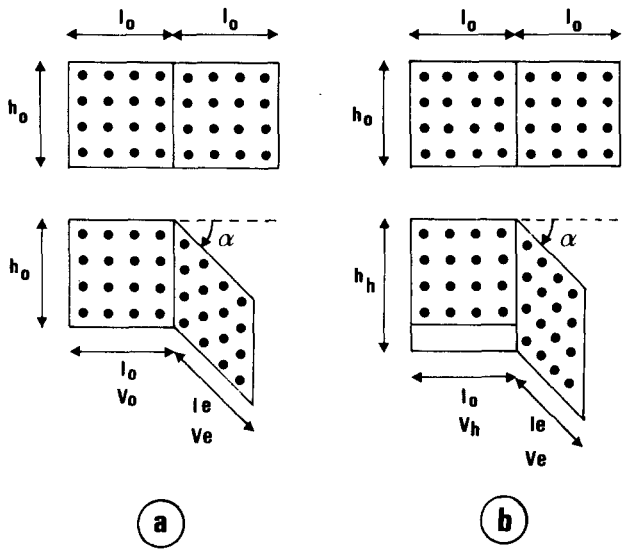

Fig. 4. Material transfer models in the limb–hinge pair of a straight-limbed fold. The limb deformation is simulated by a shear zone with volume change normal to the shear-zone walls, by loss of soluble elements. The quantity of insoluble minerals (black dots) remains constant. Two types of behaviour can be distinguished (see also Fig. 7). (a) The soluble elements leave the limb and the whole limb–hinge pair. This is known as an open system: $\Delta V = V_e - V_o$; $I_p/I_e = (1 + \Delta) = (1 + \Delta l/l_o) \cos \alpha$. (b) The soluble elements leave the limb and relocate in the hinge: this is known as a closed system: $\Delta V = V_e - V_o = V_o - V_h$; $I_p/I_e = (1 + \Delta)/(1 - \Delta) = (1 + \Delta l/l_o) \cos \alpha$.

models for material distribution by pressure-solution may be distinguished.

(i) The elements of soluble minerals leave the fold limb and the whole analysed area, by pressure-solution. The hinge represents the initial state of the rock (system said to be open on the scale of the limb–hinge pair).

(ii) The elements of soluble minerals leave the limb by pressure-solution but relocate in the hinge, in tension gashes normal to the shear zone (system said to be closed on the scale of the limb–hinge pair).

In some favourable cases, this difference can be established by observing or not observing in the hinge, traces of solution or deposition through a microscope or by cathodoluminescence (Smith & Stenstrom 1965).

The relationships between limb-volume and limb-length changes (Δ, $\Delta l/l_o$) can be established for the two models following previous assumptions and nomenclature. I_e and I_p are the insoluble contents in exposed zones (limbs) and protected zones (hinge). $\Delta M = \Delta V = \Delta S$ are the mass, volume and area changes (two dimensions) where $\Delta l = l_e - l_o$ and $\Delta V = V_e - V_o$ (l_e and V_e are the final length and volume of limb, l_o and V_o are the initial length and volume, α is the angle between limb and hinge).

In the open system, case (i)

$$I_p/I_e = V_e/V_o = (1 + \Delta) = (1 + \Delta l/l_o) \cos \alpha.$$

In the closed system, case (ii), V_h and V_e are the final volume of hinge and limb,

$$I_p/I_e = V_e/V_h = (1 + \Delta)/(1 - \Delta) = (1 + \Delta l/l_o) \cos \alpha.$$

The theoretic evolution of the parameters Δ, $\Delta l/l_o$ and α are shown in Fig. 7(a) for the open system and Fig. 7(b) for the closed system. For a stated limb–hinge pair, it is sufficient to choose one of the transfer models and plot the Δ to α values to derive the fold limb elongation. The same method may be applied to shear zones with volume change. It can also be applied to a wholly coaxial deformation: the above relations can be simplified by replacing ($l_e \cos \alpha$) by l_w (exposed zone width).

APPLICATIONS TO SOME FOLD EXAMPLES

Volume change in the matrix around a buckle fold

Results. Chemical analyses of core samples from two slate layers adjacent to a folded competent layer (quartz + calcite) have been carried out (Fig. 5a). The description of the regional structural environment was given by Gratier & Vialon (1980). The fold is in a Jurassic formation (Sinemurian) on the Pont d'Oulles road to Villard-Reymond (Oisans, French Alps).

One of the layers is located just above the competent layer. Sample 9 (Fig. 5a) has been chosen to represent the initial layer composition. It comes from the assumed protected sector located near the ptygmatic fold extrados; there are no traces of solution or deposition in this particular zone. A slaty cleavage with divergent fan (Fig. 5b), mineral preferred orientation (subvertical strain axis X), and traces of solution and pressure shadows around pyrites is observed in all other samples of this layer (nos. 1–11) (Gratier & Vialon 1980). Therefore, the layer as a whole is considered an open system.

The other layer (Fig. 5a), situated further from the competent folded layer, is horizontal. Sample 14 is chosen as a reference but it does not represent the initial state as it is deformed in the same way as the whole layer, with a homogeneously dipping slaty cleavage (Fig. 5b).

As formerly described and illustrated in Fig. 2, the evolution of $R(X)$ ratios (concentration ratio of an element X between a protected zone and an exposed zone) may be analysed with respect to strain intensity (here characterized by layer dip β). Figure 2 showed that the variations in R(Fe)/R(Al), R(Ti)/R(Al) and R(K)/R(Al) ratios very seldom reach 10% and especially that these ratios do not change substantially when β increases. So these elements are distributed in minerals considered as being insoluble (muscovite, chlorite, pyrite, Ti-oxide). On the other hand, for other elements such as Mg, Ca and Si, $R(X)/R$(Al) ratios change significantly as β varies; so they are distributed in soluble minerals (quartz, calcite, dolomite) (see previous section).

The Δ value is calculated for each sample (compared with the reference sample) from the equation

$$\Delta = (\Delta M/M_o)Fd = (I_p/I_e) - 1, \text{ with } Fd = 1.$$

The evolution of the Δ values along a horizontal axis normal to the fold axis is given in Fig. 5(c). These Δ values are only relative values of volume change if the reference sample did not represent the initial state of the rocks (e.g. for the top layer with reference sample no.

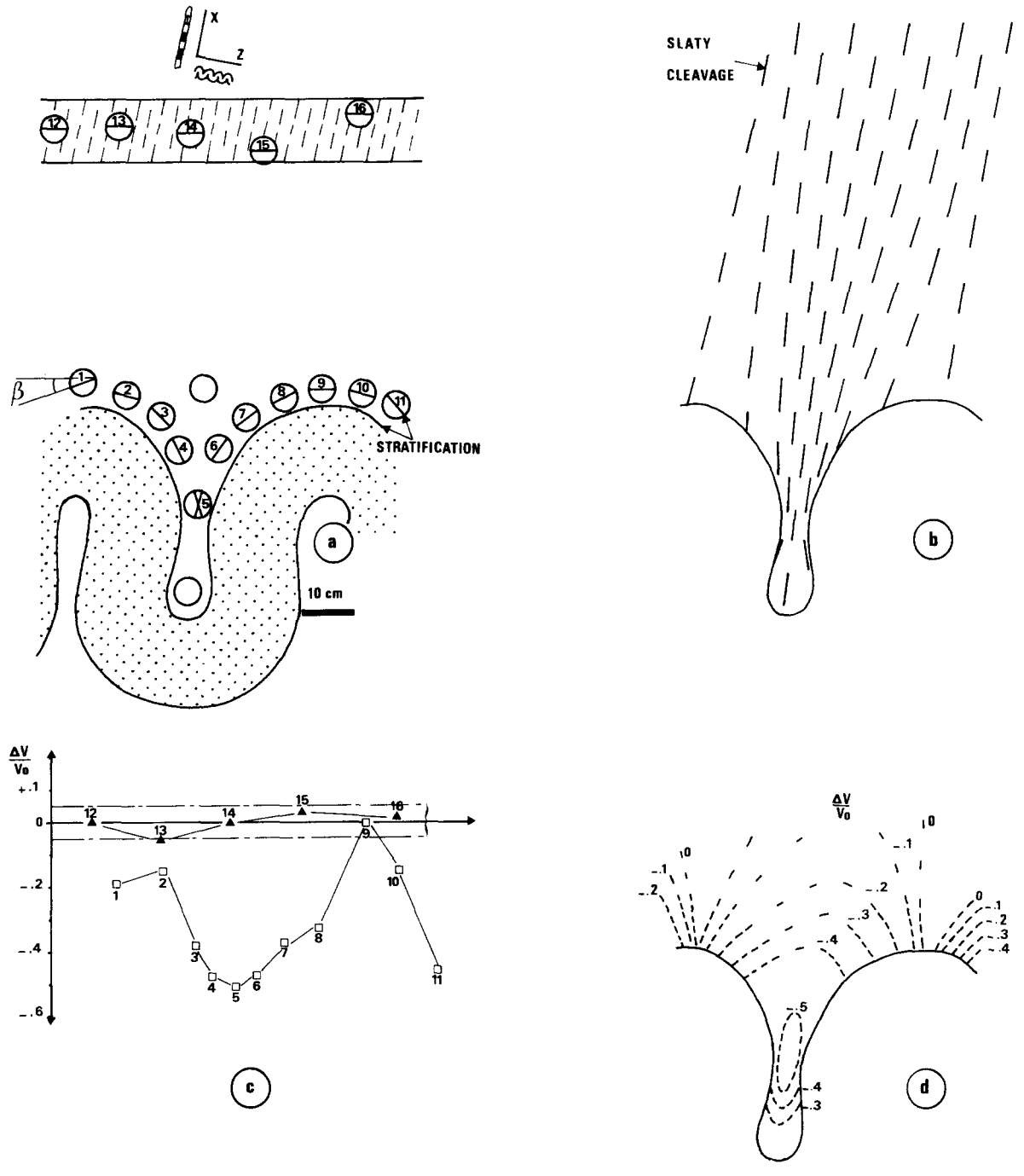

Fig. 5. Estimation of volume-change values and of their relations with finite strain values in the slaty matrix around the buckle fold of a competent layer. (a) Location of core samples, and layer dip (β) for each sample. The bottom boundary of the studied zone is the competent folded layer, the top boundary is a horizontal layer. Principle strain axes X and Z are shown (b) Dip of slaty cleavage planes on a cross-section normal to the fold axis. (c) Variations in Δ values (volume change $\Delta V/V_0$) in two layers, along a horizontal axis. Samples no. 14 (top layer) and no. 9 (bottom layer, just above the competent folded layer) are the reference zones for each layer. It will be noted that the two layers have very different behaviours. The chemical composition of the top layer (triangles) is almost homogeneous whereas that of the bottom layer (squares) reveals a substantial chemical differentiation. (d) Distribution of the Δ values in the slaty matrix, deduced from the previous values and used to calculate the finite strain values in this zone (Fig. 6b).

14). In the case of the lower layer near the ptygmatic fold, the reference sample (no. 9), showing no trace of solution and deposition, was considered representative of the initial state of this layer, so the Δ values calculated are probably not very different from the absolute volume change.

The difference of results for the two layers is apparent in Fig. 5(c). A significant spatial evolution of Δ, locally >50%, is to be observed for the lower layer. The same is not true for the top layer, in which Δ variations do not exceed 5%. Taking into account calculation inaccuracies (see previous discussion), the chemical composition of the top layer is considered as homogeneous. The Δ values from the lower layer are also plotted on the cross-section of Fig. 5(d) to illustrate the spatial variation of Δ around the ptygmatic fold.

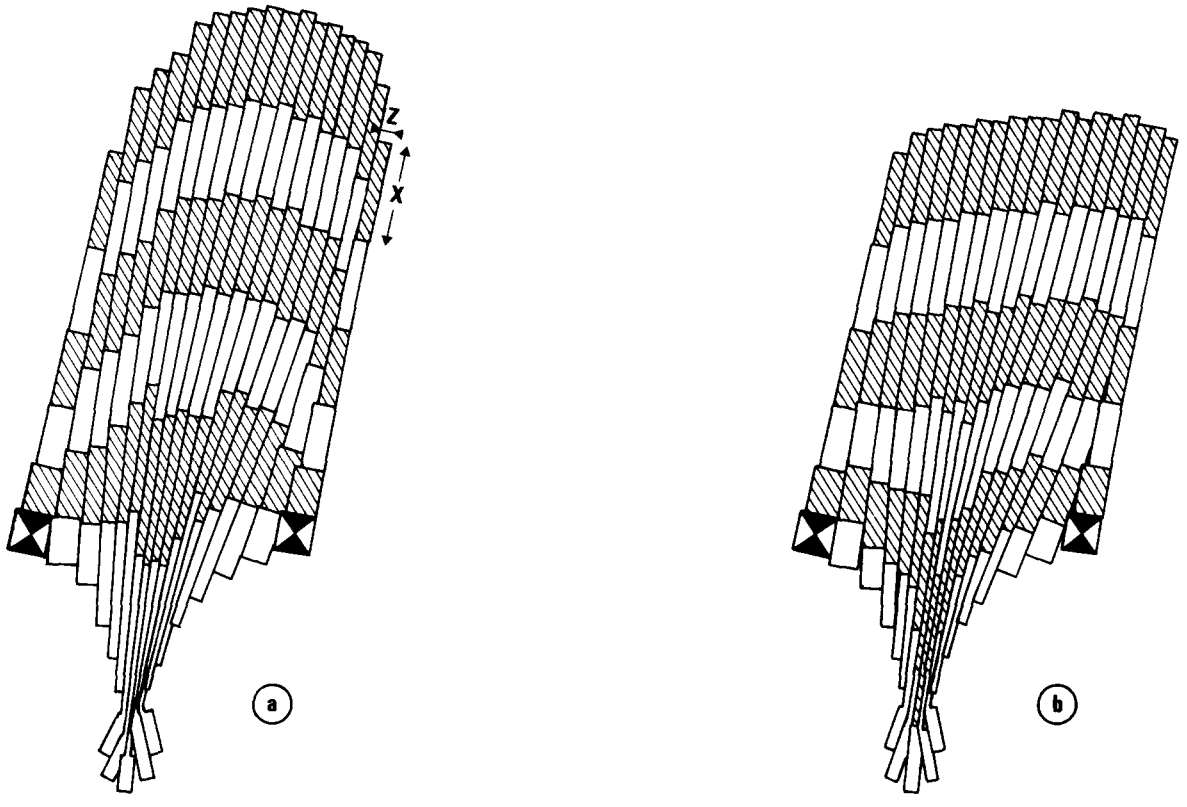

Fig. 6. Distribution of principal finite strain values X and Z. Calculation is based on finite strain values at the boundaries of the studied zone: horizontal shortening $Z = 0.4$ (unfolding of competent layer); vertical stretching (top layer) = $X = 2.5$; $Y = 1$ (truncated belemnites). The whole area is divided into 108 elements whose deformations are considered as being homogeneous. Two cases can be distinguished: (a) $\Delta = 0$ and (b) Δ = values from Fig. 5(d). The strain distribution obtained in the latter case is compatible with the observed deformed state (horizontal top layer).

Relationship to strain. Unfortunately, no fossils or other markers are to be found within the studied area. It is therefore impossible to unstrain elemental sectors to restore the initial state (Cobbold 1979). But, by assuming the most probable initial state (parallel and horizontal layers), it is possible to find finite-strain and volume-change values which are compatible within this deformed zone. Indeed, strain values at the boundaries of this zone are known. The overall horizontal shortening (Z = finite length/initial length), given by unfolding the competent layer assuming it did not become thicker during deformation, gives $Z = 0.4$. Vertical stretching (X) around the studied zone is given by measuring truncated belemnites. With some caution as to the precise significance of these values (Gratier & Vialon 1980), the results are $X = 2.5$, $Y = 1$.

Then, by means of photographs, the cleavage planes (equated with the XY planes) between the two layers are drawn. The whole area is divided into 18 subvertical stripes, taking into account the following boundary conditions for the two layers:

(i) deformation is homogeneous in the top layer $X = 2.5$, $Y = 1$, $Z = 0.4$ and consequently $\Delta = 0$;

(ii) there is no décollement at the boundary between the bottom layer and competent layer and no change in this boundary length compared with the probable initial state (horizontal layer).

Z can be estimated at any point of the deformed area by measuring the distances between the cleavage planes drawn. Then X may be calculated by dividing the subvertical stripes into six elements whose deformations are considered as homogeneous. The two elements situated above the competent layer fold extrados are not deformed: they represent the initial state (protected zones). In order to obtain X values, two cases are considered, the first by using the Δ values found through chemical analysis (Fig. 6b) and the second, by taking $\Delta = 0$ (Fig. 6a). In the latter case, a significant bend will be observed above the ptygmatic fold intrados which does not coincide with the finite deformation state. On the other hand if the calculated decrease in volume is taken into account, the top layer is found to be almost horizontal. A very slight bend is still present; it could be due to an underestimation of Δ because variations in density were neglected or due to uncertain strain values.

The volume changes calculated by comparing chemical analyses are entirely compatible with the studied strain patterns. This method, when systematically applied, could thus be used to account for some gaps and overlaps occurring when the non-deformed state is restored by the unstraining of homogeneous elements (Cobbold 1979).

Volume change between limbs and hinges in straight-limbed folds

Results. Chemical analysis have been carried out on several limb–hinge pairs of straight-limbed folds of the

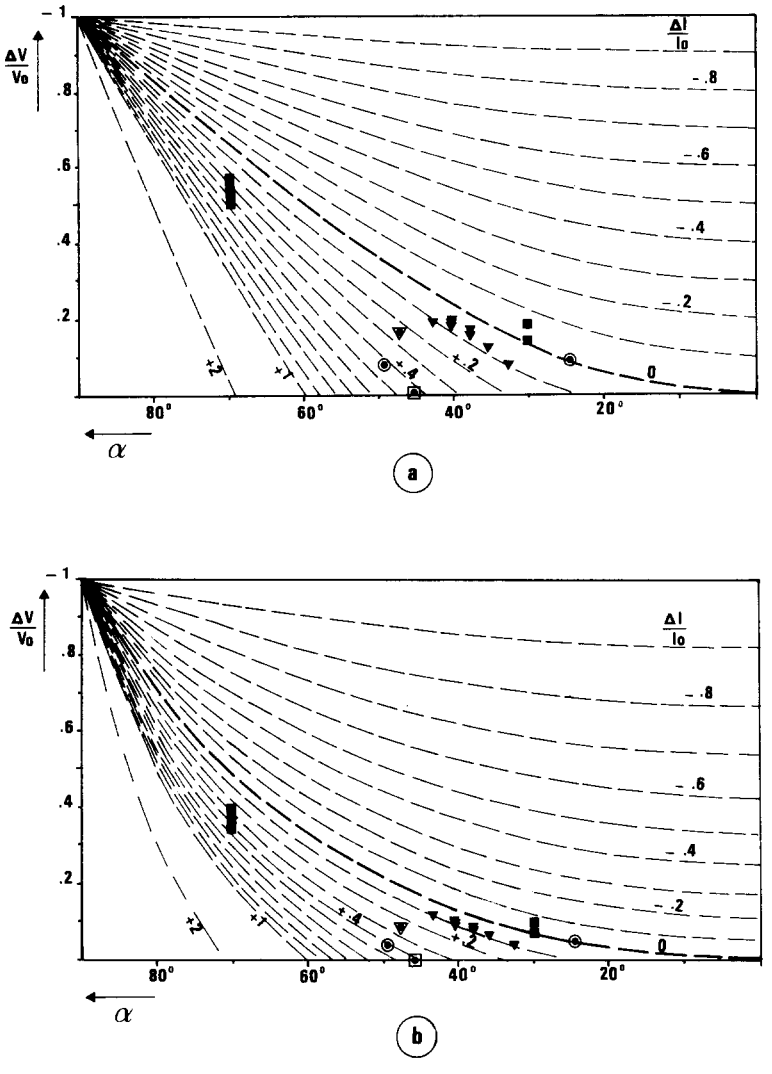

Fig. 7. Relations between Δ, $\Delta l/l_0$ and α for the two transfer models defined in Fig. 4. Δ is the volume change $\Delta V/V_0$, $\Delta l/l_0$ the change in length parallel to the layer in the fold limb and α the angle between hinge and limb. (a) is the open system, and (b) the closed system. The values obtained for various natural examples are plotted on these diagrams and discussed in the text. Each symbol represents one limb–hinge pair. See Fig. 4 for Δ calculations. Black squares: Jurassic, Col des Saisies, Savoie (also in Figs. 3b and 9a). Black triangles: Jurassic, Col du Lautaret, Hte Alpes (also in Figs. 3c and 9b). Other symbols: Jurassic, west cover of Belledonne, Isere, France.

same layer and where possible with various limb–hinge angles α as in Fig. 3. Almost all the samples have been taken from the Mesozoic cover to the external crystalline basements in the French Alps (Pelvoux, Belledonne, Mont-Blanc) (Gratier & Vialon 1980). All these folds, unlike those of the previous examples (Figs. 2 and 5) have one common feature: the presence only of crenulation cleavage (in some limbs), parallel to the limb–hinge boundary (Fig. 3). In all cases also, the hinge is taken as a reference (protected zone). As in the previous example, chemical analyses are used to distinguish between the elements remaining in the limbs and those leaving them (Fig. 3). The mineralogical composition changes are then calculated by taking as insoluble minerals those containing elements whose $R(X)/R(\mathrm{Al})$ ratios are in the range 1.1–0.9.

Δ was calculated from chemical comparative analysis with the relations:

$\Delta = (I_p/I_e) - 1$, for open systems (Fig. 7a),
$\Delta = (I_p - I_e)/(I_p + I_e)$, for closed systems (Fig. 7b).

The two models were used for each limb–hinge pair. For the same pair the Δ values are then different: Δ varies from −36% (closed system) to −53% (open system) for the same fold, at $\alpha = 70°$ (black squares, Fig. 7). This large difference in Δ values for the two models underlines the necessity to determine the true transfer model (open or closed system for each hinge–limb pair). However the relations between α and $\Delta l/l_0$ are not modified by the choice of the model of transfer (see Fig. 7). Although the open system would seem more probable from the microscopic observations of the hinges (no clear traces of solution or deposition for most of the samples), the Δ values have been plotted on the two diagrams (Fig. 7) nevertheless.

Discussion. First, a good correlation of the Δ values can be observed for various hinge–limb pairs of the same layer, with identical α angles (clusters of black squares and black triangles). Various behaviours in the relations between Δ, $\Delta l/l_0$ and α are also to be noticed, which may be summarized as four different types:

(1) Limb volume decrease may be high (−20%) even

when the elongation parallel to the strata is zero or hardly significant, whichever transfer model is chosen. $\Delta l/l_0$ is about +5% to +10% for some samples (Col du Lautaret) with α angles between 32.5 and 42.5° (black triangles). $\Delta l/l_0$ is zero for other folds. The dominant mechanism of deformation must be a mass transfer process by pressure-solution with either diffusion from limb to hinge in a closed system (Gresens 1966), or infiltration of fluid which transports matter away from the fold in an open system.

(2) Volume change may also be zero (white square with point). Limb deformation is a stretching parallel to the layer, proportional to the increase of α value with fold amplification, without mass transfer in the hinge–limb pair. Of course the fact that there is only one fold with this behaviour is not statistically representative. Folding may often occur without volume change, but the examples presented here were chosen by selecting folds with apparent difference between hinge and limb.

(3) The Δ values may also vary with the angle α (black squares); the finite elongations $\Delta l/l_0$ vary from −5% (shortening) with $\alpha = 30°$, to +40% (stretching), with $\alpha = 70°$. In this case with a large release of matter, the limbs probably show a slight shortening parallel to the stratification, at the beginning of folding, and a stretching parallel to the stratification, with fold amplification and increasing α values.

(4) Relatively significant stretching (25–45%) occurs for relatively low values of Δ. Such a case is an intermediate case between the preceding ones (white circle and triangle with points).

Fold examples—general discussion

The results show that Δ and $\Delta l/l_0$ values may vary considerably in otherwise similar geometrical structures. The effect of some of the important factors will be briefly analysed.

(1) Comparison of different deformed samples with crenulation cleavage (Figs. 3 and 7), and with almost identical pressure and temperature conditions (determined by the microthermometric study of the fluid inclusions of crystals in tension gashes normal to cleavage, Bernard *et al.* 1977), show two important factors. First is the influence of the initial rock composition. Using the Δ values of Fig. 7, and extrapolating these values for identical $\alpha = 45°$, the volume change increases from 10 to 30% when the initial soluble mineral content varies from 60 to 80%. Second is the influence of another parameter which may be less easy to characterize and yet is perhaps more important: the structure of the rock (Voll 1960, Robin 1979). It is to be noted that for identical compositions and geometry, volume changes are more substantial as rocks show a well-developed initial layering (small micaceous shale layers).

(2) Comparisons of deformed samples with different cleavages at various pressure and temperature conditions, show differences (Gratier 1979) in classifying the various minerals into mobility characteristics (Figs. 8 and 9). In the case of a slaty cleavage, quartz is more mobile than calcite and dolomite (Fig. 8). In the case of a crenulation cleavage, it is the reverse (Fig. 9). In such cases, temperature probably affects the solubility of these minerals, slaty cleavage showing evidence of higher temperature (Bernard *et al.* 1977, Jenatton 1981) and crenulation cleavage lower temperature. A systematic study of this effect could perhaps determine if the slowest process during pressure-solution is always the transport or if dissolution or crystallization could also be the rate controlling process (Fisher & Elliot 1973, Raj 1982, and preliminary results, on experimental solution-deposition, by the author).

The volume-change values of each mineral may also change during deformation. For example (Fig. 8), for a low layer dip, calcite and dolomite are not mobile whereas for a steeper dip, their mobility tends to be equal or superior to that of the quartz.

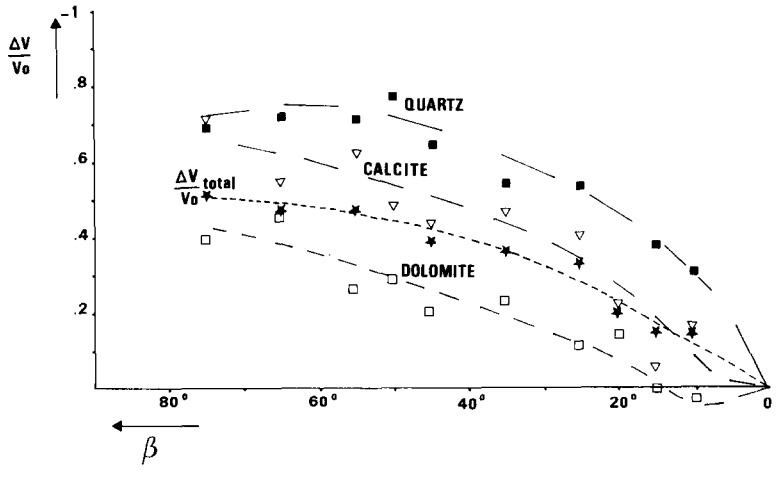

Fig. 8. Comparison of the behaviour of the various soluble minerals by pressure-solution and evolution as deformation increases (increases in limb dip β). For the same layer the relative mobility of quartz, calcite and dolomite varies with the increase in deformation (increased β). The volume change Δ of each mineral is $\Delta V/V_0 = (I_p/I_e)(M_e/M_p) - 1$, for the open system, chosen here. The sketch of the fold is given in Fig. 5(a); an axial plane slaty cleavage is associated with the fold. See Fig. 9 for comparison with folds with crenulation cleavage.

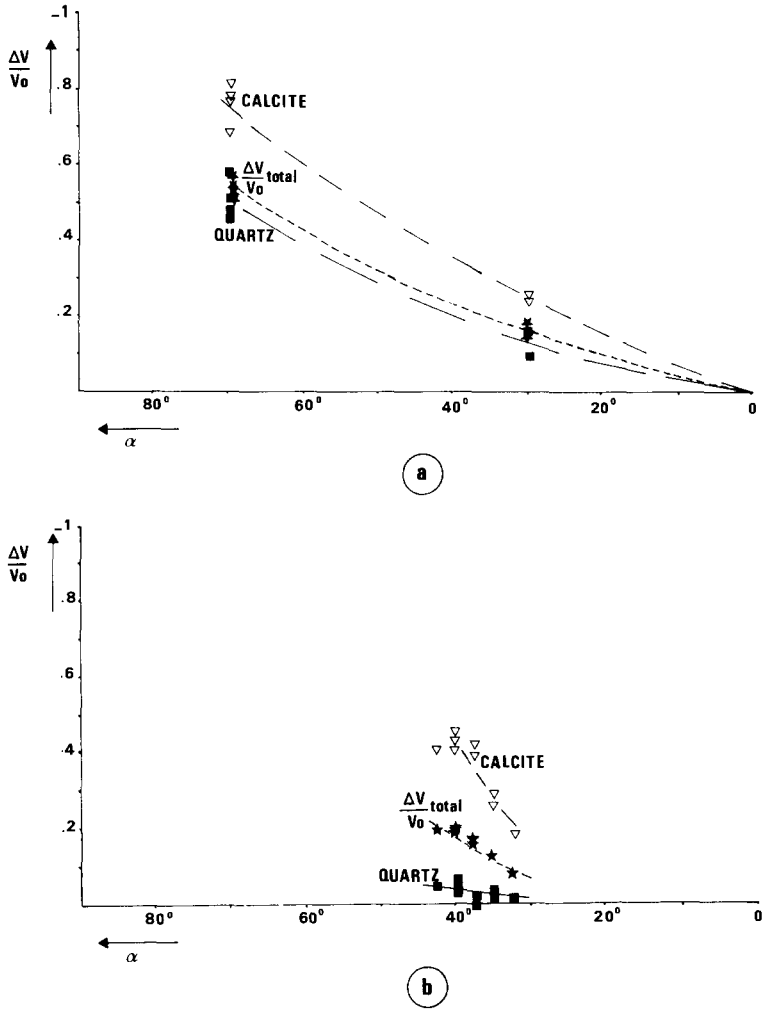

Fig. 9. Comparison of the behaviour of the various soluble minerals by pressure-solution and evolution as deformation increases (increase in limb–hinge angle α). Same Δ calculations as in Fig. 8. The folds are those of Figs. 3 and 7; (a) is the black square in Fig. 7 and (b) the black triangles in Fig. 7. Crenulation cleavage is associated with the folds. See Fig. 8 for comparison with fold with slaty cleavage.

The influence of these various parameters on the elements' relative mobilities is currently being studied on a larger number of samples.

CONCLUSIONS

The proposed method allows estimates of volume changes (Δ) to be made between various sectors of the same layer heterogeneously deformed by pressure-solution with mass transfer.

From simple observations the validity of the assumptions required to calculate Δ and the magnitude of transfers due to other processes (recrystallizations) may be checked.

In the analysis of slates around a ptygmatic fold, the calculated Δ decrease values may reach 50% and are compatible with the general strain pattern.

In the study of various limb-hinge pairs of straight-limbed folds, the relations between Δ, $\Delta l/l_0$ (limb elongation) and α (limb–hinge angle) are determined. These variables probably depend on the following parameters: temperature and pressure, the initial composition and structure (anisotropy) of the rocks, and the evolution of these factors with progressive deformation.

This work also demonstrates that the volume of the closed system for mass transfer by pressure-solution could be estimated. Therefore, the distance of transfer may also be estimated. This could lead to ideas on the mechanism of this transfer (diffusion, infiltration or coupled process) and also on the mechanism of pressure-solution. A larger number of analyses are needed, which are being carried out currently.

Acknowledgements—I would like to thank A. M. Sabatini, G. Buffet, F. Thouvenot, P. Vialon, G. Vivier for their help and S. H. Treagus, R. Kerrich and the anonymous reviewer for the improvement of the manuscript. This work received financial support from the Tectonophysics ATP no. 3694.

REFERENCES

Barrouquere, G., Deramond, J., Majeste-Menjoulas, C. & Soula, J. C. 1969. Interprétation microtectonique de la structure 'griotte'. *C. r. hebd. Séanc. Acad. Sci., Paris* 431–433.

Bernard, D., Gratier, J. P. & Pécher, A. 1977. Application de la microthermométrie des inclusions fluides des cristaux syn-cinématiques à un problème tectonique. *C. r. somm. Séanc. Soc. géol. Fr.* **5**, 284–288.

Boulter, C. A. & Raheim, A. 1974. Variation in Si^{4+} content of phengites through a three stage deformation sequence. *Contr. Miner. Petrol.* **48**, 57–71.

Buffet, G. 1981. Variabilité des caractères splitiques et magmatiques du volcanisme alcalin triasique du massif des Ecrins Pelvoux (Alpes Françaises). Thèse d'Etat Grenoble.

Caron, J. M., Kienast, J. R. & Triboulet, C. 1981. High pressure–low temperature metamorphism and polyphase Alpine deformation at Sant'Andrea di Cotone (Eastern Corsica, France). *Tectonophysics* **78**, 419–451.

Cobbold, P. R. 1979. Removal of finite deformation using strain trajectories. *J. Struct. Geol.* **1**, 67–72.

Cobbold, P. R. & Percevault, M. N. 1983. Spatial integration of strains using finite elements. *J. Struct. Geol.* **5**, 299–305.

Delair, J. & Leroux, C. 1978. Méthodes de quantification de la disparition de matière au niveau de stylolites tectoniques et mécanismes de la déformation cassante des calcaires. *Bull. Soc. géol. Fr.*, 7 *Ser.* **20**, 137–144.

Durney, D. W. 1972. Solution transfer, an important geological deformation mechanism. *Nature, Lond.* **235**, 315–317.

Etheridge, M. A. & Hobbs, B. E. 1974. Chemical and deformational controls on recrystallization of mica. *Contr. Miner. Petrol.* **43**, 111–124.

Fisher, G. W. & Elliott, D. 1973. Criteria for quasi-steady diffusion and local equilibrium in metamorphism. In: *Geochemical Transport and Kinetics* (edited by Hoffman, A. W., Giletti, B. J., Yoder, H. S. & Yund, R. A.) Carnegie Inst. of Washington, 231–241.

Gratier, J. P. 1976. Déformation et changement de volume dans un marbre à stylolithes de la région de rabat (Maroc). *Bull. Soc. géol. Fr.*, 7 *Ser.* **18**, 1461–1471.

Gratier, J. P. 1979. Mise en évidence de relations entre changement de composition chimique et intensité de déformation dans les roches à schistosité. *Bull. Soc. géol. Fr.*, 7 *Ser.* **21**, 95–104.

Gratier, J. P. 1982. Approche expérimentale et naturelle de la déformation des roches par dissolution–cristallisation avec transfert de matière. *Bull. Mineral.* **105**, 201–300.

Gratier, J. P. & Vialon, P. 1980. Deformation pattern in a heterogeneous material: folded and cleaved sedimentary cover immediately overlying a crystalline basement (Oisans, French Alps). *Tectonophysics* **65**, 151–180.

Gray, D. R. 1977. Differentiation associated with discrete crenulation cleavage. *Lithos* **10**, 89–101.

Gresens, R. L. 1966. The effect of structurally produced pressure gradients on diffusion in rocks. *J. Geol.* **74**, 307–321.

Jenatton, L. 1981. Microthermométrie des inclusions fluides des cristaux associés à l'ouverture de fentes alpines. Thèse de 3è Cycle, Grenoble.

Kerrich, R. 1977. An historical review and synthesis of research on pressure solution. *Zentbl. Miner. Geol. Paläont.* **5/6**, 512–550.

Knipe, R. J. 1981. The interaction of deformation and metamorphism in slates. *Tectonophysics* **78**, 249–273.

Percevault, M. N. & Cobbold, P. R. 1982. Mathematical removal of regional ductile strains in Central Brittany: evidence for wrench tectonics. *Tectonophysics* **82**, 317–328.

Raj, R. 1982. Creep in polycristalline aggregate by matter transport through a liquid phase. *J. geophys. Res.* **87**, 4731–4739.

Ramsay, J. G. 1967. *Folding and Fracturing of Rocks*. McGraw-Hill, New York.

Ramsay, J. G. 1980. Shear zone geometry: a review. *J. Struct. Geol.* **2**, 82–99.

Robin, P. I. 1979. Theory of metamorphic segregation and related processes. *Geochim. cosmochim. Acta* **43**, 1587–1600.

Schwerdtner, W. M. 1977. Geometric interpretation of regional strain analyses. *Tectonophysics* **39**, 515–531.

Smith, J. V. & Stenstrom, R. C. 1965. Electron excited luminescence as a petrologic tool. *J. Geol.* **73**, 627–635.

Stephansson, O. 1974. Stress induced diffusion during folding. *Tectonophysics* **22**, 233–251.

Stephens, M. B., Glasson, M. J. & Keays, R. R. 1979. Structural and chemical aspects of metamorphic layering development in meta sediments from Clunes, Australia. *Am. J. Sci.* 279–160.

Vernon, R. H. 1977. Microfabric of mica aggregates in partly recrystallized biotite. *Contr. Mineral. Petrol.* **61**, 175–185.

Voll. G. 1960. New work on petrofabrics. *Lpool Manchr Geol. J.* **2**, 503–567.

Wilson, C. J. L. & Bell, I. A. 1979. Deformation of biotite and muscovite: optical microstructure. *Tectonophysics* **58**, 179–200.

Williams, P. F. 1972. Development of metamorphic layering and cleavage in low grade metamorphic rocks at Bermagui, Australia. *Am. J. Sci.* **272**, 1–47.